RAA 2017 Vol. **17** No. **2**, 14 (7pp) doi: 10.1088/1674–4527/17/2/14

http://www.raa-journal.org *http://iopscience.iop.org/raa*

***R**esearch in*
***A**stronomy and*
***A**strophysics*

Modeling the redshift and energy distributions of fast radio bursts

Xiao-Feng Cao, Ming Xiao and Fei Xiao

Department of Physics and Engineering, Hubei University of Education, Wuhan 430205, China;
caoxf@mails.ccnu.edu.cn

Received 2016 September 6; accepted 2016 October 14

Abstract Fast radio bursts (FRBs) are one of the most mysterious astronomical phenomena nowadays. The identification of their origin requires more observations in the future and, importantly, deep understandings of the existing observational data. By fitting the redshift and energy distributions of 15 Parkes FRBs, we try to derive their intrinsic energy function and the cosmic evolution of their burst rates. Specifically, while the energy function is assumed as usual to have a single-power-law form, the burst rates are considered to be proportional to the cosmic star formation rates by a redshift-dependent coefficient. Some plausible fittings are obtained, which indicate the power-law assumptions are feasible and effective. The values of the power-law indices could be used to independently constrain candidate FRB models, although parameter degeneracies still exist.

Key words: radio continuum: general

1 INTRODUCTION

Fast radio bursts (FRBs) are intense radio transients with intensities of a few to a few tens of Jansky at $\sim 1\,\mathrm{GHz}$ (Lorimer et al. 2007; Keane et al. 2012; Keane & Petroff 2015; Thornton et al. 2013; Burke-Spolaor & Bannister 2014; Spitler et al. 2014; Champion et al. 2016; Masui et al. 2015; Ravi et al. 2015). The origin of FRBs is a mystery at present because of the absence of some necessary information including their distances. It is very difficult to capture and identify the counterparts of FRBs in other electromagnetic bands due to their short millisecond durations and the low angular resolutions of present radio surveys. So far there is only one possible radio afterglow reported to be associated with an FRB, FRB 150418 (Keane & Petroff 2015). According to the afterglow observation, a candidate host galaxy was selected for this FRB, which indicates that FRBs can have a cosmological origin. However, such a unique observation is still under debate (e.g., Williams & Berger 2016; Li & Zhang 2016; Zhang 2016). As argued, the claimed radio afterglow could just be a coincident scintillating steady radio source or an active galactic nucleus flare. In any case, in spite of the lack of direct distance measurement, the cosmological origin of FRBs is still strongly suggested by their anomalously high dispersion measures (DMs; $\sim 300-1600\,\mathrm{cm^{-3}\,pc}$), which seem too large to be accounted for in the Milky Way in view of their high Galactic latitudes. By considering the primary contribution to the DMs from the intergalactic medium (IGM), the redshifts of FRBs can be inferred to be $z\sim 0.2-1.5$. As a result, the isotropic-equivalent total energy released during an FRB can be estimated to be within the range $\sim 10^{39}-10^{41}$ erg.

Based the cosmological origin scenario, a dozen FRB models have been proposed, such as hyperflares of soft gamma-ray repeaters (Popov & Postnov 2010), synchrotron maser emission from relativistic, magnetized shocks due to magnetar flares (Lyubarsky 2014), supergiant pulses from pulsars (Cordes & Wasserman 2016), collisions of asteroids with neutron stars (Geng & Huang 2015; Dai et al. 2016), collapses of supra-massive neutron stars to black holes at several thousand to a million years old (Falcke & Rezzolla 2014) or at birth (Zhang 2014), inspiral or mergers of double neutron stars (Wang et al. 2016; Totani 2013), mergers of binary white dwarfs (Kashiyama et al. 2013), oscillations of superconducting cosmic string loops (Vachaspati 2008; Cai et al. 2012; Yu et al. 2014), etc. All of these models could basically explain the primary characteristics of FRBs such as their short durations and large energy releases. Distinguishing these models undoubtedly requires more observational

evidence. One existing useful constraint comes from the observational event rate of FRBs, which is estimated to be on the order of $\sim 10^4\,\mathrm{sky}^{-1}\,\mathrm{day}^{-1}$. In addition to a general calculation of the total event rate, Yu et al. (2014) suggested using the number distribution of FRBs at different redshift to strengthen the observational constraint on the models. As a first attempt, they investigated the superconducting cosmic string burst model and successfully minimized the free space of the model parameters, even though only a very small number of FRBs could be used then. In the past several years, the number of FRBs has continuously increased, which makes it possible to implement some more general statistical studies (Bera et al. 2016; Caleb et al. 2016; Li et al. 2016; Katz 2016; Oppermann et al. 2016). In this paper, by considering that most FRB models are related to neutron star systems, we relate the burst rates of FRBs with cosmic star formation history by a coefficient which exhibits a power-law function of redshift. Furthermore, we introduce a power-law intrinsic energy function. Then, following Yu et al. (2014), we constrain the indices of these power laws by simultaneously fitting the redshift and energy distributions of FRBs. The obtained results should be satisfied and accounted for by any candidate model, which is therefore beneficial for testing and distinguishing different FRB models in future works.

2 OBSERVATIONAL DISTRIBUTIONS OF FRBS

Since the first discovery of FRB 010125 by Lorimer et al. (2007) with Parkes, so far totally 17 FRBs have been recorded, including two events, FRB 121102 and FRB 110523, detected by the Arecibo and Green Bank Telescopes, respectively. In addition, observations of FRB 121102 indicated there were 16 repeating bursts, which was a surprise, making it completely different from the other events (Spitler et al. 2016; Scholz et al. 2016; Wang & Yu 2016; Li et al. 2016). In the following statistics, we only take the 15 Parkes FRBs (as listed in Table 1) into account, in order to avoid complications due to different telescope parameters. The data are taken from the website *http://www.astronomy.swin.edu.au/pulsar/frbcat/* (see Petroff et al. 2016 and references therein).

Excluding FRB 150418, no independent redshift measurement has been achieved for any other FRBs. Therefore, as usual, we derive redshift z from the DMs of the FRBs. In principle, the DM of an FRB can be contributed by the Milky Way, the IGM, the host galaxy and the FRB source itself. In view of the large uncertainty in the origin of an FRB, we generally assume the DM contribution from the FRB source is insignificant, although such an assumption may not always be correct (e.g. Yu 2014). The DMs in the Milky Way can be calculated from the NE2001 model (Cordes & Lazio 2002) and here we take a typical value of $\mathrm{DM_{MW}} = 60\ \mathrm{pc\ cm^{-3}}$ for directions away from the Galactic plane ($b > 5^\circ$). For a host galaxy, a representative value of $100\ \mathrm{pc\ cm^{-3}}$ is used to give $\mathrm{DM_{host}}(z) = 100/(1+z)\,\mathrm{pc\ cm^{-3}}$. Finally, the IGM contribution is calculated by

$$\mathrm{DM_{IGM}}(z) = \int_0^z \frac{cn_\mathrm{e}(z')}{(1+z')^2 H(z')} dz', \qquad (1)$$

where $n_\mathrm{e}(z) = 2.1\times10^{-7}(1+z)^3\,\mathrm{cm^{-3}}$ is the number density of free electrons and

$$H(z) = H_0[(1+z)^3\Omega_{m,0} + \Omega_{\Lambda,0}]^{1/2}$$

with cosmological parameters of

$$H_0 = 71\,\mathrm{km\,s^{-1}\,Mpc^{-1}},$$

$\Omega_{m,0} = 0.27$ and $\Omega_{\Lambda,0} = 0.73$. The inferred redshifts of the Parkes FRBs are listed in Table 1. With these redshifts, we can estimate the isotropic energy releases of the FRBs by

$$E = 4\pi d_c(z)^2(1+z)\Delta\nu S_\nu \Delta t_\mathrm{obs} k(z), \qquad (2)$$

where $d_c(z) = c\int_0^z H(z')^{-1}dz'$ is the comoving distance, $\Delta\nu = 0.4$ GHz is the frequency bandwidth of the Parkes survey, and S_ν and Δt_obs are the average flux density and the pulse width of the FRBs respectively. The correction factor k converts the energy from the observational frequency band into a common emitting frequency range of $\nu_a < \nu < \nu_b$ for all FRBs. By assuming a power-law spectrum of $S_\nu \propto \nu^{-\beta}$, the $k-$correction factor can be calculated by

$$k(z) = (1+z)^{\beta-1}({\nu_b}^{1-\beta} - {\nu_a}^{1-\beta})/({\nu_2}^{1-\beta} - {\nu_1}^{1-\beta}).$$

Finally we plot the FRB distribution in the $z-E$ plane in Figure 1, where the $k-$correction is not included.

3 MODELING THE FRB DISTRIBUTIONS

3.1 FRB Event Rate Density

As the most straightforward consideration, the distribution of number of FRBs at a given redshift could reflect the cosmic evolution of their event rate and also the number of their progenitors, which could provide an informative and stringent constraint on the candidate progenitor models of FRBs. For example, Yu et al. (2014) tested the superconducting cosmic string burst model by fitting the redshift distribution of four FRBs. Here, we are mainly concerned with the more traditional FRB models that are

Table 1 Observational Data and Inferred Redshifts and Energies

FRB	DM ($\mathrm{pc\,cm^{-3}}$)	Pulse width (ms)	Fluence (Jy ms)	Redshift	Energy (10^{40} erg)
010125	790(3)	$9.40^{+0.20}_{-0.20}$	2.82	0.65	1.22
010621	745(10)	7	2.87	0.60	1.10
010724	375	5	>150.00	0.24	7.91
090625	899.55(1)	$1.92^{+0.83}_{-0.77}$	$2.19^{+2.10}_{-1.12}$	0.75	1.24
110220	944.38(5)	$5.60^{+0.10}_{-0.10}$	$7.28^{+0.13}_{-0.13}$	0.80	4.58
110626	723.0(3)	1.4	0.56	0.58	0.20
110703	1103.6(7)	4.3	2.15	0.95	2.00
120127	553.3(3)	1.1	0.55	0.42	0.10
121002	1629.18(2)	$5.44^{+3.50}_{-1.20}$	$2.34^{+4.46}_{-0.77}$	1.48	5.01
130626	952.4(1)	$1.98^{+1.20}_{-0.44}$	$1.47^{+2.45}_{-0.50}$	0.81	0.94
130628	469.88(1)	$0.64^{+0.13}_{-0.13}$	$1.22^{+0.47}_{-0.37}$	0.33	0.13
130729	861(2)	$15.61^{+9.98}_{-6.27}$	$3.43^{+6.55}_{-1.81}$	0.72	1.77
131104	779(1)	2.08	2.33	0.64	0.98
140514	562.7(6)	$2.80^{+3.50}_{-0.70}$	$1.32^{+2.34}_{-0.50}$	0.43	0.24
150418	776.2(5)	$0.80^{+0.30}_{-0.30}$	$1.76^{+1.32}_{-0.81}$	0.63	0.74

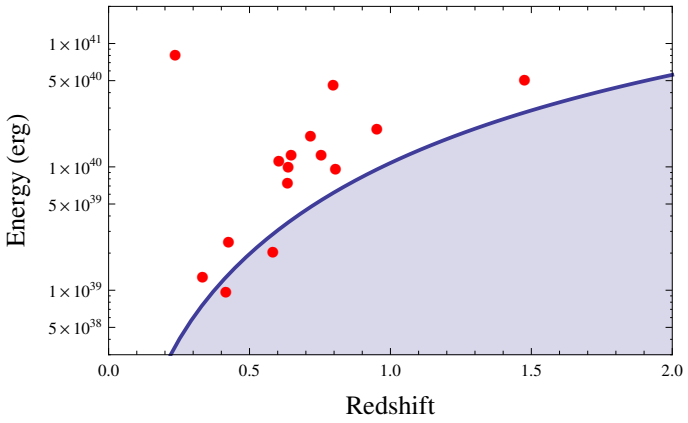

Fig. 1 The distribution of 15 Parkes FRBs in the $z - E$ plane. The *solid line* represents the observational energy threshold of the Parkes telescope corresponding to a minimum signal-to-noise ratio of $n_{\min} = 10$.

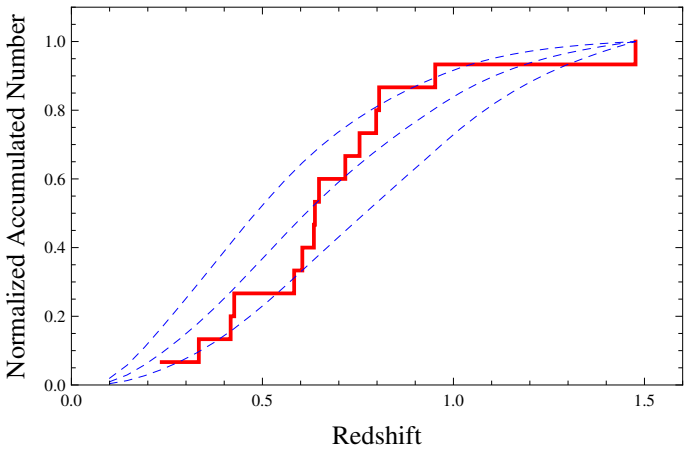

Fig. 2 Fittings to the normalized cumulative distribution of redshifts of FRBs (*solid histograms*) with Equation (5) for $\alpha = -5,\ -7$ and -9 from bottom to top (*dashed lines*), respectively, where the observational threshold is not taken into account.

usually related to neutron star systems. Thus we assume that the burst rate density of FRBs at redshift z, $\dot{R}(z)$, is proportional to the star formation rate density at the same redshift, $\rho_*(z)$. However, in general, the constant of proportionality between these two rates is assumed to evolve with redshift as a power-law function

$$\dot{R}(z) \propto (1+z)^{\alpha}\dot{\rho}_*(z), \tag{3}$$

where the index α is a free parameter. The physical reason determining the evolution of the coefficient is complicated, which could be due to some particular requirements on FRB progenitors such as for long gamma-ray bursts (GRBs) (Langer & Norman 2006; Cao et al. 2011), due to some time delays in short GRBs (Wanderman & Piran 2015), or due to an evolutional energy function (cf. see Tan et al. 2013 for long GRBs). So, the actual expression of the coefficient could deviate very far from the power-law form. In any case, at present, the simple treatment in Equation (3) is convenient and empirically effective. By introducing the cosmic star formation history (Hopkins & Beacom 2006)

$$\dot{\rho}_*(z) \propto \begin{cases} (1+z)^{3.44}, & z < 0.97, \\ (1+z)^{-0.26}, & 0.97 \leq z < 4, \end{cases} \tag{4}$$

with $\dot{\rho}_*(0) = 0.02\,\mathrm{M_\odot\,yr^{-1}\,Mpc^{-3}}$, the cumulative number of FRBs for redshifts $< z$ can be given by

$$N_{<z}^{\rm obs} = \mathcal{T}\frac{\mathcal{A}}{4\pi}\int_{z_{\rm min}}^{z}\dot{R}(z')\frac{dV(z')}{1+z'}, \tag{5}$$

where $\mathcal{T}$ is the duration of each pointed observation (Thornton et al. 2013), $\mathcal{A}$ is the sky area of the survey, the factor $(1+z)$ represents the cosmological time dilation for an observed rate and $dV(z)/dz = 4\pi d_c(z)^2 c/H(z)$ is the comoving volume element. The minimum redshift for the above integration is set at $z = 0.05$, which corresponds to a DM of $200\,\mathrm{pc\,cm^{-3}}$ above which current FRB searches are conducted.

In Figure 2, we confront the observational normalized redshift distribution with theoretical curves computed by Equation (5) with varying α, which demonstrates that a very strong evolution in $-5 < \alpha < -9$ is required for the number decay at high redshifts. It is seemingly indicated that FRBs could mainly (even only) happen at low redshifts of $z < 1$, which may somewhat reflect some intrinsic physical suppression effects. Nevertheless, in any case, this decay/evolution must also be, at least partially, caused by telescope selection due to a flux threshold, which is however neglected in Equation (5).

3.2 Telescope Threshold

An FRB can be detected by a radio telescope when the signal-to-noise ratio is higher than a certain threshold. The signal-to-noise ratio can be defined by dividing the average flux density S_ν of the signal by the rms flux density fluctuation ΔS due to the telescope's system noise. The system noise can be given by

$$\Delta S = T_{\rm sys}/(G\sqrt{\Delta\nu\Delta t_{\rm obs}N_{\rm pol}}),$$

where $T_{\rm sys}$, G and $N_{\rm pol}$ are the system temperature, the antenna gain of the primary beam and the number of polarizations, respectively (Bera et al. 2016; Caleb et al. 2016). The integration time for the observation $\Delta t_{\rm obs}$ can be taken as the pulse width of the FRB. For a fiducial value of $\Delta t_{\rm obs} = 1\,\mathrm{ms}$, we have $[\Delta S]_{1\rm ms} = 0.05\,\mathrm{Jy}$. Then, the observational energy threshold for FRBs can be estimated by

$$E_{\rm th}(z) = 4\pi d_c(z)^2(1+z)\Delta\nu n_{\rm min}\Delta S\Delta t_{\rm obs}k(z), \tag{6}$$

where $n_{\rm min}$ is the characteristic minimum signal-to-noise ratio below which the ability to identify an FRB signal decreases drastically.

Due to the system noise $\Delta S \propto \Delta t_{\rm obs}^{-1/2}$, the energy threshold is dependent on pulse width as $E_{\rm th} \propto \Delta t_{\rm obs}^{1/2}$. Thus, it is necessary to clarify the redshift dependence of pulse width for determining the threshold. For an FRB with an intrinsic pulse width $\Delta t_{\rm burst}$ located at redshift z, its observed duration is influenced and determined by cosmic expansion over time, residual dispersion and scattering in the intervening medium, i.e.,

$$\Delta t_{\rm obs}(z) = \sqrt{\Delta t_{\rm burst}^2(1+z)^2 + \Delta t_{\rm DM}^2 + \Delta t_{\rm scat}^2}. \tag{7}$$

Specifically, for a telescope with central frequency ν_0 and single frequency channel width $\Delta\nu_c$, the residual dispersion broadening across the single frequency channel can be approximately given by

$$\Delta t_{\rm DM}(z) \approx 8.3\times10^6\,\mathrm{DM}(z)\Delta\nu_c/\nu_0^3\ \mathrm{ms}$$

for $\Delta\nu_c/\nu_0 \ll 1$. For Parkes, $\nu_0 = 1382$ MHz and $\Delta\nu_c = 390$ kHz. The theory of scattering broadening is unclear, e.g., see Xu & Zhang (2016) for a comprehensive investigation. Here for a simple analytical expression, we adopt the temporal smearing equation for IGM turbulence from Macquart & Koay (2013) as

$$\Delta t_{\rm scat}(z) = \frac{k_{\rm scat}\left[1-\sqrt{z/(1+z)}\right]}{\nu_0^4(1+z)} \times \int_0^z \frac{H_0}{H(z')}dz' \int_0^z \frac{H_0(1+z')^3}{H(z')}dz', \tag{8}$$

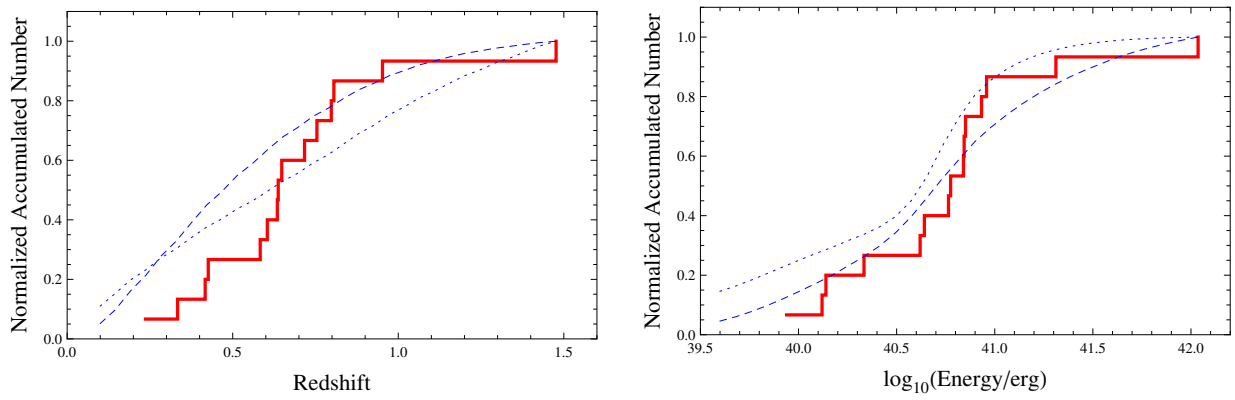

Fig. 3 Example fittings to the normalized cumulative distributions of redshifts and energies of FRBs for $\alpha = -5$ (*dashed line*) and $\alpha = 0$ (*dotted line*) and a spectral index $\beta = -2$. The value of γ is taken according to Eq. (11).

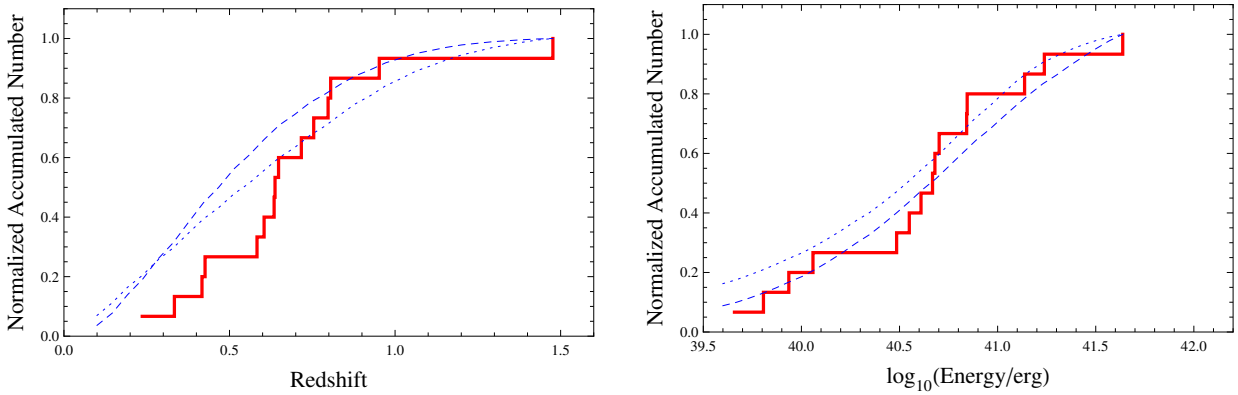

Fig. 4 The same as Fig. 3 but for $\beta = 0$.

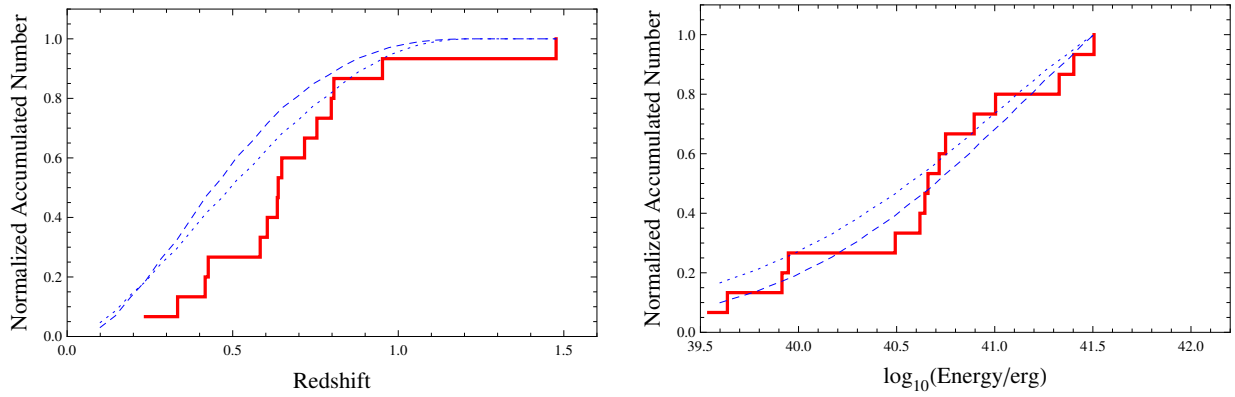

Fig. 5 The same as Fig. 3 but for $\beta = 2$.

where the normalization coefficient

$$k_{\rm scat} = 4.2 \times 10^{13}\ {\rm ms\,MHz^4}$$

and a corresponding fiducial intrinsic width of

$$\Delta t_{\rm burst} = 1.3\ {\rm ms}$$

are both obtained by fitting the distribution of the pulse widths of all FRBs. However, the contribution to the scattering broadening from the host galaxy medium is ignored arbitrarily, even though this contribution could sometimes be dominant (Xu & Zhang 2016).

Finally, by substituting Equation (7) into (6), we can get the energy threshold of the Parkes telescope survey as a function of redshift. This threshold is represented by the solid line in Figure 1, in which the uncertain $k-$correction is not taken into account. As shown, such a threshold is very consistent with the distribution of data.

3.3 Confronting with Observations

By considering telescope selection by the energy threshold $E_{\rm th}$, the calculation of cumulative numbers of FRBs in redshift range $< z$ can be changed to

$$N^{\rm obs}_{<z} = \mathcal{T}\frac{\mathcal{A}}{4\pi}\int_{z_{\rm min}}^{z}\int_{E_{\rm th}(z)}^{E_{\rm max}}\Phi(E)\dot{R}(z')dE\frac{dV(z')}{1+z'}, \quad (9)$$

where $E_{\rm max} = 10^{42}$ erg is taken and an energy function $\Phi(E)$ is introduced to describe the intrinsic energy distribution of FRBs, which is assumed to have a power-law form of $\Phi(E) \propto E^{-\gamma}$. Here the energy function is taken to be constant and its possible redshift dependence has been included in the coefficient $(1+z)^{\alpha}$. Moreover, the cumulative number for energy range $< E$ is given by

$$N^{\rm obs}_{<E} = \mathcal{T}\frac{\mathcal{A}}{4\pi}\int_{E_{\rm min}}^{E}\int_{z_{\rm min}}^{z_{\rm max}}\Phi(E)\dot{R}(z')\frac{dV(z')}{1+z'}dE, \quad (10)$$

where the minimum energy is taken as $E_{\rm th}(0.05)$. The maximum redshift $z_{\rm max}$ is determined by $\max(z_{\rm th}, 1.9)$, where the value of $z_{\rm th}$ is solved from the equation $E = E_{\rm th}(z_{\rm th})$ and the value of 1.9 corresponds to the maximum DM$= 2000\,{\rm pc\,cm^{-3}}$ below which FRB searches are conducted.

Using Equations (9) and (10) we can fit the cumulative distributions of number of FRBs in both redshift and energy. However, due to the simplicity of the model and lack of data, it is not easy, or even possible, to obtain a very precise fitting to the observed distributions. By using a χ^2 test, we find a rough empirical relationship among the model parameters α, β and γ of

$$\begin{aligned}\gamma \sim &(0.150 - 0.017\beta + 0.001\beta^2)\alpha \\ &+ (2.117 + 0.193\beta + 0.017\beta^2),\end{aligned} \quad (11)$$

with which some relatively good fittings to the observations can be found. Some plausible examples are presented in Figures 3, 4 and 5 for spectral indices $\beta = -2$, 0 and 2, respectively. By comparing with Figure 2, the evolution effect could be significantly suppressed and even the non-evolving case can also not be ruled out. Nevertheless, the model parameters are still highly degenerate.

4 SUMMARY AND DISCUSSIONS

By introducing a power-law energy function and assuming that the burst rates of FRBs track cosmic star formation history by a redshift-dependent coefficient, we try to fit the redshift and energy distributions of FRBs, where the selection effect due to the telescope threshold and the spectral correction to the observed fluxes are taken into account. As a result, we obtain some plausible fittings with an empirical relationship among the three power-law indices. This indicates that the simple power-law empirical expressions for the burst rates and energy function are workable and effective, just as are some analogical studies of gamma-ray bursts (e.g., Cao et al. 2011; Yu et al. 2012). The obtained values of the power-law indices can provide some independent and useful constraints on the candidate models of FRBs. For example, if the case of $\alpha = 0$ can be finally confirmed by future observations, it would be indicative that the phenomena associated with FRBs are probably due to the death of some peculiar main-sequence stars. In this case, a model relying on collapses of newly-born neutron stars could be favored.

Acknowledgements The authors appreciate Yun-Wei Yu for encouraging us to do this work and for his valuable help in the calculations. This work is supported by the National Natural Science Foundation of China (Grant Nos. 11303010 and 11473008).

References

Bera, A., Bhattacharyya, S., Bharadwaj, S., Bhat, N. D. R., & Chengalur, J. N. 2016, MNRAS, 457, 2530
Burke-Spolaor, S., & Bannister, K. W. 2014, ApJ, 792, 19
Cai, Y.-F., Sabancilar, E., & Vachaspati, T. 2012, Phys. Rev. D, 85, 023530
Caleb, M., Flynn, C., Bailes, M., et al. 2016, MNRAS, 458, 708
Cao, X.-F., Yu, Y.-W., Cheng, K. S., & Zheng, X.-P. 2011, MNRAS, 416, 2174
Champion, D. J., Petroff, E., Kramer, M., et al. 2016, MNRAS, 460, L30
Cordes, J. M., & Lazio, T. J. W. 2002, astro-ph/0207156
Cordes, J. M., & Wasserman, I. 2016, MNRAS, 457, 232
Dai, Z. G., Wang, J. S., Wu, X. F., & Huang, Y. F. 2016, ApJ, 829, 27
Falcke, H., & Rezzolla, L. 2014, A&A, 562, A137
Geng, J. J., & Huang, Y. F. 2015, ApJ, 809, 24
Hopkins, A. M., & Beacom, J. F. 2006, ApJ, 651, 142
Kashiyama, K., Ioka, K., & Mészáros, P. 2013, ApJ, 776, L39

Katz, J. I. 2016, ApJ, 818, 19
Keane, E. F., & Petroff, E. 2015, MNRAS, 447, 2852
Keane, E. F., Stappers, B. W., Kramer, M., & Lyne, A. G. 2012, MNRAS, 425, L71
Langer, N., & Norman, C. A. 2006, ApJ, 638, L63
Li, L., Huang, Y., Zhang, Z., Li, D., & Li, B. 2016, arXiv:1602.06099
Li, Y., & Zhang, B. 2016, arXiv:1603.04825
Lorimer, D. R., Bailes, M., McLaughlin, M. A., Narkevic, D. J., & Crawford, F. 2007, Science, 318, 777
Lyubarsky, Y. 2014, MNRAS, 442, L9
Macquart, J.-P., & Koay, J. Y. 2013, ApJ, 776, 125
Masui, K., Lin, H.-H., Sievers, J., et al. 2015, Nature, 528, 523
Oppermann, N., Connor, L. D., & Pen, U.-L. 2016, MNRAS, 461, 984
Petroff, E., Barr, E. D., Jameson, A., et al. 2016, PASA, 33, 45
Popov, S. B., & Postnov, K. A. 2010, in Evolution of Cosmic Objects through their Physical Activity, eds. H. A. Harutyunian, A. M. Mickaelian, & Y. Terzian, 129
Ravi, V., Shannon, R. M., & Jameson, A. 2015, ApJ, 799, L5
Scholz, P., Spitler, L. G., Hessels, J. W. T., et al. 2016, arXiv:1603.08880
Spitler, L. G., Cordes, J. M., Hessels, J. W. T., et al. 2014, ApJ, 790, 101
Spitler, L. G., Scholz, P., Hessels, J. W. T., et al. 2016, Nature, 531, 202
Tan, W.-W., Cao, X.-F., & Yu, Y.-W. 2013, ApJ, 772, L8
Thornton, D., Stappers, B., Bailes, M., et al. 2013, Science, 341, 53
Totani, T. 2013, PASJ, 65, L12
Vachaspati, T. 2008, Physical Review Letters, 101, 141301
Wanderman, D., & Piran, T. 2015, MNRAS, 448, 3026
Wang, F. Y., & Yu, H. 2016, arXiv:1604.08676
Wang, J.-S., Yang, Y.-P., Wu, X.-F., Dai, Z.-G., & Wang, F.-Y. 2016, ApJ, 822, L7
Williams, P. K. G., & Berger, E. 2016, ApJ, 821, L22
Xu, S., & Zhang, B. 2016, arXiv:1608.03930
Yu, Y.-W. 2014, ApJ, 796, 93
Yu, Y.-W., Cheng, K. S., Chu, M. C., & Yeung, S. 2012, J. Cosmol. Astropart. Phys., 7, 023
Yu, Y.-W., Cheng, K.-S., Shiu, G., & Tye, H. 2014, J. Cosmol. Astropart. Phys., 11, 040
Zhang, B. 2014, ApJ, 780, L21
Zhang, B. 2016, ApJ, 822, L14